Published in final edited form as:
Biosens Bioelectron. 2016 May 15; 79: 644–649. doi:10.1016/j.bios.2015.12.102.

Ultrasensitive detection of influenza viruses with a glycan-based impedimetric biosensor

András Hushegyi[1], **Dominika Pihíková**[1], **Tomáš Bertók**[1], **Vojtech Adam**[2], **René Kizek**[2], and **Jan Tkac**[1,*]

[1]Department of Glycobiotechnology, Institute of Chemistry, Slovak Academy of Sciences, Dubravska cesta 9, 845 38 Bratislava, Slovakia

[2]Department of Chemistry and Biochemistry, Mendel University in Brno, Zemedelska 1, 613 00 Brno, Czech Republic

Abstract

An ultrasensitive impedimetric glycan-based biosensor for reliable and selective detection of inactivated, but intact influenza viruses H3N2 was developed. Such glycan-based approach has a distinct advantage over antibody-based detection of influenza viruses since glycans are natural viral receptors with a possibility to selectively distinguish between potentially pathogenic influenza subtypes by the glycan-based biosensors. Build-up of the biosensor was carefully optimized with atomic force microscopy applied for visualization of the biosensor surface after binding of viruses with the topology of an individual viral particle H3N2 analyzed. The glycan biosensor could detect a glycan binding lectin with a limit of detection (LOD) of 5 aM. The biosensor was finally applied for analysis of influenza viruses H3N2 with LOD of 13 viral particles in 1 μl, what is the lowest LOD for analysis of influenza viral particles by the glycan-based device achieved so far. The biosensor could detect H3N2 viruses selectively with a sensitivity ratio of 30 over influenza viruses H7N7. The impedimetric biosensor presented here is the most sensitive glycan-based device for detection of influenza viruses and among the most sensitive antibody or aptamer based biosensor devices.

Keywords

Biosensors; electrochemical impedance spectroscopy; glycans; influenza virus; lectins; SAMs

1 Introduction

Glycans as complex carbohydrates are involved in many pathological and physiological processes in living organisms including immune response, tumor metastasis, infection by bacteria/viruses, inflammation, molecular recognition and cell signaling (Cecioni et al. 2015; Park et al. 2013; Pritchard et al. 2015; Reichardt et al. 2013; Rogowski et al. 2015; Varki 2009; Wesener et al. 2015). Better understanding of glycan biorecognition in such processes has been deeply studied in recent years since such information can be then applied for

*Corresponding author: Jan.Tkac@savba.sk, Tel.: +421 2 5941 0263, Fax: +421 2 5941 0222.

Europe PMC Funders Author Manuscripts

development of novel therapeutic and diagnostic approaches; and for design of novel potent vaccines, as well (Alley et al. 2013; Bournazos et al. 2014; Burton et al. 2012; Dalziel et al. 2014; Macauley et al. 2014; Medina and García-Sastre 2011; Rouvinski et al. 2015).

From a structural point of view, glycans form a dense layer on the surface of various cell types called glycocalyx, literarily meaning sugar coat (*glykys*=sweet, *kalyx*=husk) (Hushegyi and Tkac 2014). Such a glycan coat is involved in cell-cell recognition and host-pathogen interactions since glycans as more complex and information rich molecules compared to DNA and proteins can effectively store and code information, working as an identity card for a particular cell type (Song et al. 2015). The density of glycans on the cell surface membrane is immense, with over 10 million glycan molecules containing terminal sialic acid (i.e. reaching concentration of 100 mM) (Cummings and Pierce 2014).

Glycans present on the surface of the host cells have an important role in an initial stage of viral infections involving various influenza subtypes. Influenza A viruses can infect humans, birds, horses, pigs and marine mammals. The infection is realized through virus cell wall glycoproteins called hemagglutinins (HA) and neuraminidases (NA). Influenza A viruses are categorized according to the type of HA and NA proteins (i.e. H1N1, H3N2, etc.) present on the viral surface with 18 HA and 11 NA subtypes described so far (Watanabe et al. 2014). The first step in the infection process is an interaction between HA and host glycans terminated in sialic acid (de Graaf and Fouchier 2014). Avian influenza viruses prefer to bind to sialic acid which is linked to galactose via α2-3 linkage. On the other hand, human influenza viruses prefer to bind to sialic acid, which is linked to galactose with α2-6 linkage. There also exist influenza viruses (for example H3N2) which are able to make interactions with glycans terminated in α2-3 and α2-6 linked sialic acids (Air 2014).

Fluorescent glycan biochips with glycans printed at high density on glass slides have been successfully applied to study interaction of glycans with glycan binding proteins or with bacterial and viral particles in a highly parallel way (Arthur et al. 2014; Blixt and Westerlind 2014; Cummings and Pierce 2014; Geissner et al. 2014; Laurent et al. 2008; Stencel-Baerenwald et al. 2014; Svarovsky and Joshi 2014). Biochips however have distinct disadvantages i.e. a need to label glycoproteins or bacteria/viruses, what can compromise a biorecognition process affecting reliability of detection (Gemeiner et al. 2009). Biosensors working in a label-free mode not requiring presence of any label can solve this problem. Moreover, some transducing mechanisms such as electrochemical-based ones (Paleček et al. 2015) can work in an ultrasensitive fashion (down to aM level), what is not the case of fluorescent glycan biochips with limit of detection typically down to nM or sub nM level (Hushegyi and Tkac 2014).

In our previous work we presented an ultrasensitive impedimetric biosensor which could detect interactions between lectins or isolated influenza virus hemagglutinins and glycans, with detection limit down to aM level (Hushegyi et al. 2015). The surface chemistry for patterning of gold surface was based on a mixed SAM layer (self-assembled monolayer) consisting of 11-mercaptoundecanoic acid (MUA) and 6-mercaptohexanol (MH), resisting non-specific interaction up to 0.1 nM and allowing to control glycan density on the surface (Hushegyi et al. 2015). In this work we would like to increase selectivity of detection by the

Europe PMC Funders Author Manuscripts

glycan biosensor using surface chemistry based on a mixed SAM composed of thiols bearing oligoethylene glycol (OEG) moieties resisting non-specific interactions (Scheme S1). Moreover, the glycan biosensor was then applied in analysis of intact, but inactivated influenza viral particles in an ultrasensitive and highly selective fashion.

2 Results and discussion

2.1 Choice of SAM components

In the previous study the glycan biosensor was constructed by modification of gold electrode with a mixed SAM composed of 11-mercaptoundecanoic acid and 6-mercaptohexanol and this interfacial layer was resistant to non-specific interactions up to 0.1 nM (Hushegyi et al. 2015). Here we wanted to increase selectivity of detection by using improved surface chemistry. This is the main reason why we tested a mixed SAM composed of OEG-COOH and OEG in this study since OEG surface chemistry proved to be effective in providing non-fouling interface, previously developed by us for the SPR biosensor (Davis et al. 2009; Davis et al. 2007). In the initial set of experiments, combination of OEG thiols or aliphatic thiols terminated in –COOH and –OH with a variable chain length was tested. The following combinations i.e. binary and ternary thiol mixtures were analyzed with various ratio between components: 1. HS-$(CH_2)_{10}$-COOH and HS-$(CH_2)_8$-EG_2-OH; 2. HS-$(CH_2)_8$-EG_2-OCH_2-COOH and HS-$(CH_2)_8$-OH; 3. HS-$(CH_2)_{10}$-COOH, HS-$(CH_2)_8$-EG_3-OH and HS-$(CH_2)_8$-OH; 4. HS-$(CH_2)_8$-EG_2-OCH_2-COOH and OEG; 5. HS-$(CH_2)_8$-EG_2-OCH_2-COOH and OEG; 6. HS-$(CH_2)_{10}$-COOH, OEG and HS-$(CH_2)_8$-OH; 7. OEG and OEG-COOH. From all these mixtures only the mixture #7 (i.e. OEG with OEG-COOH) offered moderate initial R_{CT} and easily fitted Nyquist plots, suitable for further biosensor construction.

2.2 Optimization of OEG-COOH:OEG ratio

When a proper functional (-COOH containing OEG thiol) and diluting thiol (-OH terminated OEG thiol) were selected, the first parameter being optimized was the ratio of these two thiols affecting sensitivity of the glycan biosensor towards its analyte – lectin MAA. It was proved that pure OEG-COOH SAM layer gave a large R_{CT}, which could not be determined (not shown). The best sensitivity of detection of MAA by the glycan biosensor was acquired on the interface modified by OEG-COOH and OEG with ratio of 1+5 with sensitivity value of the biosensor of (7.1±0.6) % $decade^{-1}$ and other dilution ratio of either 1+15 or 1+3 gave considerable lower sensitivity of the biosensor device (i.e. (2.0 ± 1.0) % $decade^{-1}$ or (1.8 ± 0.6) % $decade^{-1}$, respectively) (Fig. 1). Reproducibility determination for MAA lectin by the biosensor device with optimal composition of a mixed SAM layer expressed as an average RSD was 6.7% (1.6-12.4%). It is worth noting, that this average RSD value represents rather reproducibility of the biosensor device construction than assay reproducibility since measurements done in triplicate were performed by different biosensor devices. Assay reproducibility was investigated by five consecutive incubations of the biosensor device with the plain buffer as shown in our previous study (Pihikova et al. 2016) revealing RSD of 1.5% and the signal increased from an original value of R_{ct} only by 2.9% (5 incubations i.e. 100 min).

2.3 Selectivity and sensitivity of the glycan biosensor

In the subsequent experiments selectivity of the glycan biosensor was examined with one analyte – lectin MAA and two non-specific probes. The first non-specific probe was lectin DSL, which does not recognize glycan with α2,3-terminated sialic acid and the second non-specific probe was human serum albumin appearing in high abundance in human sera. Results presented in Fig. 2 proved that the glycan biosensor was able to selectively bind only its analyte – lectin MAA with sensitivity of (7.0±0.3) % decade^{-1}, while the other two proteins being non-specific probes were not recognized by the glycan biosensor in the whole concentration range examined (8 aM-0.8 nM). It is worth mentioning that calibration curve for determination of MAA by the glycan biosensor device presented in Fig. 1 and Fig. 2 were obtained with independent set of biosensor devices (prepared on a different day including electrode cleaning, patterning, activation, glycan immobilization and interaction with MAA) showing very good inter assay reproducibility (Fig. 1 and Fig. 2) and very good intra assay precision (Fig. 1 *vs.* Fig. 2) for MAA analysis. From calibration curve a limit of detection (LOD) of 5 aM for MAA was calculated as described previously (Bertok et al. 2015).

2.4 Analysis of viral particles

After obtaining preliminary information about the glycan biosensor performance, the biosensor was exposed to intact, but inactivated viral particles of influenza virus H3N2. Results shown in Fig. 3 in a form of a Nyquist plot indicate that R_{CT} of (46 ± 6) kΩ for the glycan modified biosensor surface increased to a value of (58 ± 8) kΩ after incubation of the glycan biosensor with influenza H3N2 viral particles with density of 10 viral particles in 1 μl and the R_{CT} further increased with increased concentration of influenza H3N2 viral particles up to a value of (130 ± 18) kΩ after incubation with 100,000 viral particles in 1 μl (Fig. 3). Such results suggest that the glycan biosensor could be utilized to quantitatively detect influenza H3N2 viral particles.

Further, the selectivity of the glycan biosensor to detect targeted influenza virus particles was tested. For such experiment influenza H3N2 and H7N7 viral particles were applied. Results shown in Fig. 4 indicate that the glycan biosensor can selectively detect influenza H3N2 viral particles (analyte) over influenza H7N7 viral particles (non-analyte) with a selectivity ratio of 30 (i.e. sensitivity of (81 ±6)% decade^{-1} for H3N2 vs. (2.7 ±0.6)% decade^{-1} for H7N7 influenza viruses). LOD for detection of influenza H3N2 viral particles by the glycan biosensor of 13 viral particles in 1 μl was determined as previously described (Bertok et al. 2015). H3N2 viral particles were detected by the glycan biosensor device with sufficient reproducibility expressed as an average RSD of 9.7% (1.0%-23.5%), but this value represents reproducibility of the biosensor device construction, as was stated above. Thus, the glycan biosensor constructed possesses both high sensitivity and high selectivity of analysis for influenza H3N2 viral particles, what can be applied for diagnostic purposes in the future.

2.5 AFM imaging

AFM imaging did not reveal a big difference between a mean square roughness of bare gold surface (R_q=0.74 nm) and the interface with glycan immobilized (R_q=0.80 nm), what can be

also seen in Fig. S1A and Fig. S1B. This is in a strong contrast to results shown in our previous study, where a different mixed SAM layer (MUA and MH) was employed (Hushegyi et al. 2015). Thiols with longer aliphatic chain i.e. 11 carbon for MUA and 6 carbon for MH formed a well ordered mixed SAM with thiol molecules well aligned with each other (stabilized by van der Waals forces). When, such ordered SAM layer was applied for immobilization of glycan molecule, individual glycan molecules could be seen in AFM images with R_q factor considerably higher compared to bare gold (i.e. 1.7-fold) (Hushegyi et al. 2015). It is well known that OEG-based molecules form very flexible structures and thus a mixed SAM composed of OEG-COOH and OEG will not be that well ordered also due to a short aliphatic chain (only 3 carbons) of both thiols (OEG-COOH and OEG). Moreover it can be anticipated that OEG groups can form quite multiple hydrogen bonds with glycan molecules rich in –OH functionalities. As a result, glycan immobilized on a mixed SAM composed of OEG-COOH and OEG will not be exposed to the solution phase as an extended chain. It is quite interesting that despite interaction between glycan and thiols (OEG-COOH and OEG) after addition of lectin or influenza virus particles a biospecific reaction between glycan and its glycan binding protein or whole virus was allowed. When the glycan biosensor was incubated with influenza H7N7 viral particles, only a few features could be seen in AFM images with R_q=0.68 nm (Fig. S1C) not differing from R_q of a bare gold surface (0.74 nm), revealing only a minute amount of attached biomaterial. When the glycan biosensor was incubated with its analyte influenza H3N2 viral particles R_q increased considerably to a value of 2.77 nm and the presence of a biomaterial (i.e. debris from disrupted viral particles) including viral particles can be seen (Fig. S1D). It is possible to see dark horizontal lanes in Fig. S1D, Fig. 5A and Fig. 5B at positions, where viral particles could be seen due to movement of viral particles during scanning of the surface with the AFM tip. This suggests that such biospecific interaction between immobilized glycan and viral particles is not particularly strong.

In Fig. S2A roughness of three different surfaces is visualized showing no big difference in the surface topology for bare gold surface and the surface with covalently linked glycan to a mixed SAM layer. The roughness of the interface increased considerably after incubation with influenza H3N2 viral particles. AFM analysis of individual influenza H3N2 viral particle showed that the height of the particle is approx. 23 nm with a particle width of 170 nm (Fig. S2B). Considering AFM tip convolution effect the width can be within range of 80-120 nm, what is a typical size of influenza virus particles (Amano and Cheng 2005). The height of the viral particle however does no fall within this expected range, but recently it was suggested that influenza viral particles belong to the softest viral particles ever found and that AFM tip can quite easily disrupt viral particle (Li 2012). This would also means that even though viral particle shown in Fig. S2B seems to be intact it is damaged. A similar, although not so sharp visualization of influenza virus particle, with height of ~20 nm was recently published (Wicklein et al. 2013). Further, the evidence of damaging influenza H3N2 viral particle by the AFM tip is shown in Fig. S3. From this image it is clear that features (most likely proteins) which are on the top of the viral particle are more affected/compressed compared to the features appearing on the side of the viral particle.

2.6 QCM study

QCM experiment was applied to further prove specificity of detection of influenza H3N2 viral particles over influenza H7N7 viral particles on the glycan biosensor (Fig. S4). Further analysis revealed that (4.4 ± 0.6) μg cm^{-2} of influenza H3N2 viral particles was bound on the glycan surface, while in case of influenza H7N7 viral particles only a mass density of (0.38 ± 0.05) μg cm^{-2} was bound. It is worth mentioning that a QCM setup we used, operated in a batch mode with QCM chip being at the bottom of the measuring cell. We tried to calculate surface density of influenza H3N2 viral particles on the glycan interface and by taking a molecular weight of influenza A virus of $174x10^6$ g mol^{-1} (Ruigrok et al. 1984) we found a value of $(1.5 \pm 0.2)x10^{10}$ viral particles *per* cm^2. Once we took a hard sphere model into account (Lahiri et al. 1999) we can calculate that viral particles would have the size of approx. 90 nm. This value also suggests that during AFM imaging viral particles were severely damaged, as discussed above.

2.7 Comparison of the glycan biosensor with published concepts

Here we would like to compare LOD for detection of viral particles by the glycan-based biosensor obtained in this work with other published biosensor devices. There are of course various biorecognition elements, which can be used for construction of biosensors including glycan receptors, DNA/RNA aptamers and antibodies (Cheng and Toh 2013; Gopinath et al. 2014; Hsieh et al. 2015; Krejcova et al. 2012; Krejcova et al. 2014a; Krejcova et al. 2014b; Rodrigo et al. 2014).

Glycan-based biosensors. There is only one impedimetric study for detection of influenza H1N1 viral particles published so far based on non-covalent immobilization of a disaccharide galactose-sialic acid having hydrocarbon tail (octane), which was embedded during immobilization into SAM formed from octanethiol. Such biosensor could detect H1N1 viruses down to 0.05 μg ml^{-1} (~$2x10^5$ viruses μl^{-1}) (Wicklein et al. 2013).

Glycan modified gold nanoparticles were applied for plasmonic detection of human influenza X31 virus with LOD of 0.1 μg ml^{-1} (~ $3.5x10^5$ viruses μl^{-1}) (Marín et al. 2013) and sialic acid modified gold nanoparticles were applied for colorimetric detection of influenza viral particles down to concentration of 4,500 particles μl^{-1} (Lee et al. 2013).

Optimized colorimetric detection of influenza virus particles based on a previous work (Charych et al. 1993; Reichert et al. 1995) using polymerized liposomes containing sialic acid offered LOD ~1 HAU in 250 μl (~4,000 viruses μl^{-1}) (Charych et al. 1996).

Quartz crystal microbalance glycan biosensor can provide LOD of ~$1.5x10^5$ viruses ml^{-1} (~150 viruses μl^{-1}) (Sato et al. 1999). In another study, thiolated glycans were used to prepare a QCM biochip for detection of H5N1, H5N3 and H1N3 down to a concentration of few pM (~10^6 viruses μl^{-1}) (Wangchareansak et al. 2013).

Surface plasmon resonance with immobilized sialic acid containing liposomes offers LOD down to ~0.1 pM (~$6x10^4$ viruses μl^{-1}) (Hidari et al. 2007) and a very similar LOD for analysis of influenza A virus was also achieved with SPR based on a chip with immobilized bovine brain lipid containing sialoglycolipids (Critchley and Dimmock 2004).

Antibody-based biosensors. Interferometric label-free approach with immobilized antibodies could detected influenza A viruses down to $6.0x10^9$ μl^{-1} (Gopinath et al. 2009). Immunosensor based on photonic crystal device could detect H1N1 viruses down to 3,500 particles in 1 μl (Endo et al. 2010). Field-effect transistor based device with immobilized antibodies offered LOD of 280 H5N1 viral particles μl^{-1} (Guo et al. 2013) or 29 H3N2 viral particles μl^{-1} (Shen et al. 2012). Surface plasmon resonance assisted fluorescent method with immobilized antibodies offer LOD of 200 H3N2 viruses in 1 μl (Nomura et al. 2013). Quartz crystal microbalance with immobilized antibodies could provide LOD of 640 H5N1 viruses in 1 μl (Wang and Li 2013). Surface acoustic wave sensors with immobilized antibodies can detect as low as 3,500 influenza A viruses in 1 μl (Jiang et al. 2015) and with application of gold nanoparticles down to 138 H3N2 viruses μl^{-1} (Gopinath et al. 2013). A nanocomposite based on graphene oxide in a sandwich configuration with two antibodies involved could detect 1 influenza particle in 1 μl (Yang et al. 2015) and another sandwich configuration based on formation of Ag nanoparticles could detect 23 H7N9 viruses in 1 μl (Wu et al. 2015)

Aptamer-based biosensors. Impedimetric biosensors with immobilized DNA aptamers could detect influenza A viruses (H1N1) down to 1 virus in 1 μl (Kiilerich-Pedersen et al. 2013). Quartz crystal microbalance with immobilized DNA aptamer could provide LOD of 64 H5N1 viruses in 1 μl (Wang and Li 2013). A rather sophisticated assay protocol with involvement of magnetic beads, gold nanoparticles, DNA aptamers, a lectin and an enzyme amplified detection of H5N1 viruses with ability to detect as low as 4 viral particles in 1 μl (Fu et al. 2014).

3 Conclusions

The EIS being a label-free detection mode have distinct advantages compared to fluorescent glycan biochips. The study shows that EIS with optimized interfacial glycan-based layer can provide ultrasensitive and highly selective analytical platform for analysis of glycan binding proteins and inactivated, but intact influenza viruses in a wide concentration window. The study is a solid foundation for sensitive detection of various influenza subtypes including highly infectious ones based on interaction between viruses and natural host receptors - glycans. The EIS glycan-based biosensor has potential to be integrated into an array format of analysis with an enhanced robustness of detection in a parallel way. Such an array could provide a rapid evaluation of viral pathogenicity as well as the concentration, without a need to apply highly specific, but quite expensive antibodies.

Supplementary Material

Refer to Web version on PubMed Central for supplementary material.

Acknowledgement

Funding from the Slovak research and development agency APVV-14-0753; from VEGA 2/0162/14 and 1/0229/12 is acknowledged. The research leading to these results has received funding from the European Research Council under the European Union's Seventh Framework Program (FP/2007-2013)/ERC Grant Agreement no 311532. We would like to thank Petr Michálek a Hana Buchtelová for technical assistance. This publication is the result of the project implementation: Centre for materials, layers and systems for applications and chemical processes under

extreme conditions – Stage I, ITMS No.: 26240120007 supported by the Research & Development Operational Programe funded by the ERDF.

References

Air GM. Curr Opin Virol. 2014; 7:128–133. [PubMed: 25061947]

Alley WR, Mann BF, Novotny MV. Chem Rev. 2013; 113:2668–2732. [PubMed: 23531120]

Amano Y, Cheng Q. Anal Bioanal Chem. 2005; 381:156–164. [PubMed: 15592819]

Arthur CM, Cummings RD, Stowell SR. Curr Opin Chem Biol. 2014; 18:55–61. [PubMed: 24486647]

Bertok T, Šedivá A, Filip J, Ilcikova M, Kasak P, Velic D, Jane E, Mravcová M, Rovenský J, Kunzo P, Lobotka P, et al. Langmuir. 2015; 31:7148–7157. [PubMed: 26048139]

Blixt O, Westerlind U. Curr Opin Chem Biol. 2014; 18:62–69. [PubMed: 24487061]

Bournazos S, Klein F, Pietzsch J, Seaman, Michael S, Nussenzweig, Michel C, Ravetch, Jeffrey V. Cell. 2014; 158:1243–1253. [PubMed: 25215485]

Burton DR, Poignard P, Stanfield RL, Wilson IA. Science. 2012; 337:183–186. [PubMed: 22798606]

Cecioni S, Imberty A, Vidal S. Chem Rev. 2015; 115:525–561. [PubMed: 25495138]

Charych D, Cheng Q, Reichert A, Kuziemko G, Stroh M, Nagy JO, Spevak W, Stevens RC. Chem Biol. 1996; 3:113–120. [PubMed: 8807836]

Charych DH, Nagy JO, Spevak W, Bednarski MD. Science. 1993; 261:585–588. [PubMed: 8342021]

Cheng MS, Toh C-S. Analyst. 2013; 138:6219–6229. [PubMed: 24043121]

Critchley P, Dimmock NJ. Biorg Med Chem. 2004; 12:2773–2780.

Cummings RD, Pierce JM. Chem Biol. 2014; 21:1–15. [PubMed: 24439204]

Dalziel M, Crispin M, Scanlan CN, Zitzmann N, Dwek RA. Science. 2014; 343:37.doi: 10.1126/science.1235681

Davis JJ, Tkac J, Humphreys R, Buxton AT, Lee TA, Ko Ferrigno P. Anal Chem. 2009; 81:3314–3320. [PubMed: 19320493]

Davis JJ, Tkac J, Laurenson S, Ko Ferrigno P. Anal Chem. 2007; 79:1089–1096. [PubMed: 17263340]

de Graaf M, Fouchier RAM. EMBO J. 2014; 33:823–841. [PubMed: 24668228]

Endo T, Ozawa S, Okuda N, Yanagida Y, Tanaka S, Hatsuzawa T. Sens Actuat B: Chem. 2010; 148:269–276.

Fu Y, Callaway Z, Lum J, Wang R, Lin J, Li Y. Anal Chem. 2014; 86:1965–1971. [PubMed: 24180352]

Geissner A, Anish C, Seeberger PH. Curr Opin Chem Biol. 2014; 18:38–45. [PubMed: 24534751]

Gemeiner P, Mislovicova D, Tkac J, Svitel J, Patoprsty V, Hrabarova E, Kogan G, Kozar T. Biotechnol Adv. 2009; 27:1–15. [PubMed: 18703130]

Gopinath SCB, Awazu K, Fons P, Tominaga J, Kumar PKR. Anal Chem. 2009; 81:4963–4970. [PubMed: 19453160]

Gopinath SCB, Awazu K, Fujimaki M, Shimizu K, Shima T. PLoS One. 2013; 8:e69121. [PubMed: 23874887]

Gopinath SCB, Tang TH, Chen Y, Citartan M, Tominaga J, Lakshmipriya T. Biosens Bioelectron. 2014; 61:357–369. [PubMed: 24912036]

Guo D, Zhuo M, Zhang X, Xu C, Jiang J, Gao F, Wan Q, Li Q, Wang T. Anal Chim Acta. 2013; 773:83–88. [PubMed: 23561910]

Hidari K, Shimada S, Suzuki Y, Suzuki T. Glycoconjugate J. 2007; 24:583–590.

Hsieh K, Ferguson BS, Eisenstein M, Plaxco KW, Soh HT. Acc Chem Res. 2015; 48:911–920. [PubMed: 25785632]

Hushegyi A, Bertok T, Damborsky P, Katrlik J, Tkac J. Chem Commun. 2015; 51:7474–7477.

Hushegyi A, Tkac J. Anal Methods. 2014; 6:6610–6620. [PubMed: 27231487]

Jiang Y, Tan CY, Tan SY, Wong MSF, Chen YF, Zhang L, Yao K, Gan SKE, Verma C, Tan Y-J. Sens Actuat B: Chem. 2015; 209:78–84.

Kiilerich-Pedersen K, Daprà J, Cherré S, Rozlosnik N. Biosens Bioelectron. 2013; 49:374–379. [PubMed: 23800609]

Krejcova L, Hynek D, Adam V, Hubalek J, Kizek R. Int J Electrochem Sci. 2012; 7:10779–10801.

Krejcova L, Hynek D, Michalek P, Milosavljevic V, Kopel P, Zitka O, Konecna M, Kynicky J, Adam V, Hubalek J, Kizek R, et al. Int J Electrochem Sci. 2014a; 9:3440–3448.

Krejcova L, Nejdl L, Rodrigo MAM, Zurek M, Matousek M, Hynek D, Zitka O, Kopel P, Adam V, Kizek R. Biosens Bioelectron. 2014b; 54:421–427. [PubMed: 24296063]

Lahiri J, Isaacs L, Tien J, Whitesides GM. Anal Chem. 1999; 71:777–790. [PubMed: 10051846]

Laurent N, Voglmeir J, Flitsch SL. Chem Commun. 2008; 37:4400–4412.

Lee C, Gaston MA, Weiss AA, Zhang P. Biosens Bioelectron. 2013; 42:236–241. [PubMed: 23208092]

Li, S. Atomic force microscopy study on the mechanics of influenza viruses and liposomes. Georg-August-Universität Göttingen; 2012.

Macauley MS, Arlian BM, Rillahan CD, Pang P-C, Bortell N, Marcondes MCG, Haslam SM, Dell A, Paulson JC. J Biol Chem. 2014; 289:35149–35158. [PubMed: 25368325]

Marín MJ, Rashid A, Rejzek M, Fairhurst SA, Wharton SA, Martin SR, McCauley JW, Wileman T, Field RA, Russell DA, et al. Org Biomol Chem. 2013; 11:7101–7107. [PubMed: 24057694]

Medina RA, García-Sastre A. Nat Rev Microbiol. 2011; 9:590–603. [PubMed: 21747392]

Nomura, K-i; Gopinath, SCB.; Lakshmipriya, T.; Fukuda, N.; Wang, X.; Fujimaki, M. Nat Commun. 2013; 4:2855. [PubMed: 24335751]

Paleček E, Tkáč J, Bartošík M, Bertók T, Ostatná V, Paleček J. Chem Rev. 2015; 115:2045–2108. [PubMed: 25659975]

Park S, Gildersleeve JC, Blixt O, Shin I. Chem Soc Rev. 2013; 42:4310–4326. [PubMed: 23192235]

Pihikova D, Belicky S, Kasak P, Bertok T, Tkac J. Analyst. 2016; doi: 10.1039/C1035AN02322J

Pritchard LK, Spencer DIR, Royle L, Bonomelli C, Seabright GE, Behrens AJ, Kulp DW, Menis S, Krumm SA, Dunlop DC, Crispin DJ, et al. Nat Commun. 2015; 6doi: 10.1038/ncomms8479

Reichardt NC, Martín-Lomas M, Penadés S. Chem Soc Rev. 2013; 42:4358–4376. [PubMed: 23303404]

Reichert A, Nagy JO, Spevak W, Charych D. J Am Chem Soc. 1995; 117:829–830.

Rodrigo MAM, Zitka O, Krejcova L, Hynek D, Masarik M, Kynicky J, Heger Z, Adam V, Kizek R. Int J Electrochem Sci. 2014; 9:3431–3439.

Rogowski A, Briggs JA, Mortimer JC, Tryfona T, Terrapon N, Lowe EC, Basle A, Morland C, Day AM, Zheng HJ, Rogers TE. Nat Commun. 2015; 6doi: 10.1038/ncomms8481

Rouvinski A, Guardado-Calvo P, Barba-Spaeth G, Duquerroy S, Vaney MC, Kikuti CM, Navarro Sanchez ME, Dejnirattisai W, Wongwiwat W, Haouz A, Girard-Blanc C, et al. Nature. 2015; 520:109–113. [PubMed: 25581790]

Ruigrok RWH, Andree PJ, Hooft Van Huysduynen RAM, Mellema JE. J Gen Virol. 1984; 65:799–802. [PubMed: 6561234]

Sato T, Ishii M, Ohtake F, Nagata K, Terabayashi T, Kawanishi Y, Okahata Y. Glycoconjugate J. 1999; 16:223–227.

Shen F, Wang J, Xu Z, Wu Y, Chen Q, Li X, Jie X, Li L, Yao M, Guo X, Zhu T, et al. Nano Lett. 2012; 12:3722–3730. [PubMed: 22731392]

Song X, Heimburg-Molinaro J, Smith DF, Cummings RD. Glycoconjugate J. 2015; 32:465–473.

Stencel-Baerenwald JE, Reiss K, Reiter DM, Stehle T, Dermody TS. Nat Rev Microbiol. 2014; 12:739–749. [PubMed: 25263223]

Svarovsky SA, Joshi L. Anal Methods. 2014; 6:3918–3936.

Varki, A. Essentials of Glycobiology. Cold Spring Harbor Laboratory Press; Cold Spring Harbor, N.Y: 2009.

Wang RH, Li YB. Biosensors & Bioelectronics. 2013; 42:148–155. [PubMed: 23202345]

Wangchareansak T, Sangma C, Ngernmeesri P, Thitithanyanont A, Lieberzeit PA. Anal Bioanal Chem. 2013; 405:6471–6478. [PubMed: 23715677]

Watanabe T, Watanabe S, Maher EA, Neumann G, Kawaoka Y. Trends Microbiol. 2014; 22:623–631. [PubMed: 25264312]

Wesener DA, Wangkanont K, McBride R, Song XZ, Kraft MB, Hodges HL, Zarling LC, Splain RA, Smith DF, Cummings RD, Paulson JC, et al. Nat Struct Mol Biol. 2015; 22:603–610. [PubMed: 26148048]

Wicklein B, del Burgo MÁM, Yuste M, Carregal-Romero E, Llobera A, Darder M, Aranda P, Ortín J, del Real G, Fernández-Sánchez C, Ruiz-Hitzky E. Adv Funct Mater. 2013; 23:254–262.

Wu Z, Zhou CH, Chen JJ, Xiong CC, Chen Z, Pang DW, Zhang ZL. Biosens Bioelectron. 2015; 68:586–592. [PubMed: 25643598]

Yang ZH, Zhuo Y, Yuan R, Chai YQ. Biosens Bioelectron. 2015; 69:321–327. [PubMed: 25791337]

Europe PMC Funders Author Manuscripts

Europe PMC Funders Author Manuscripts

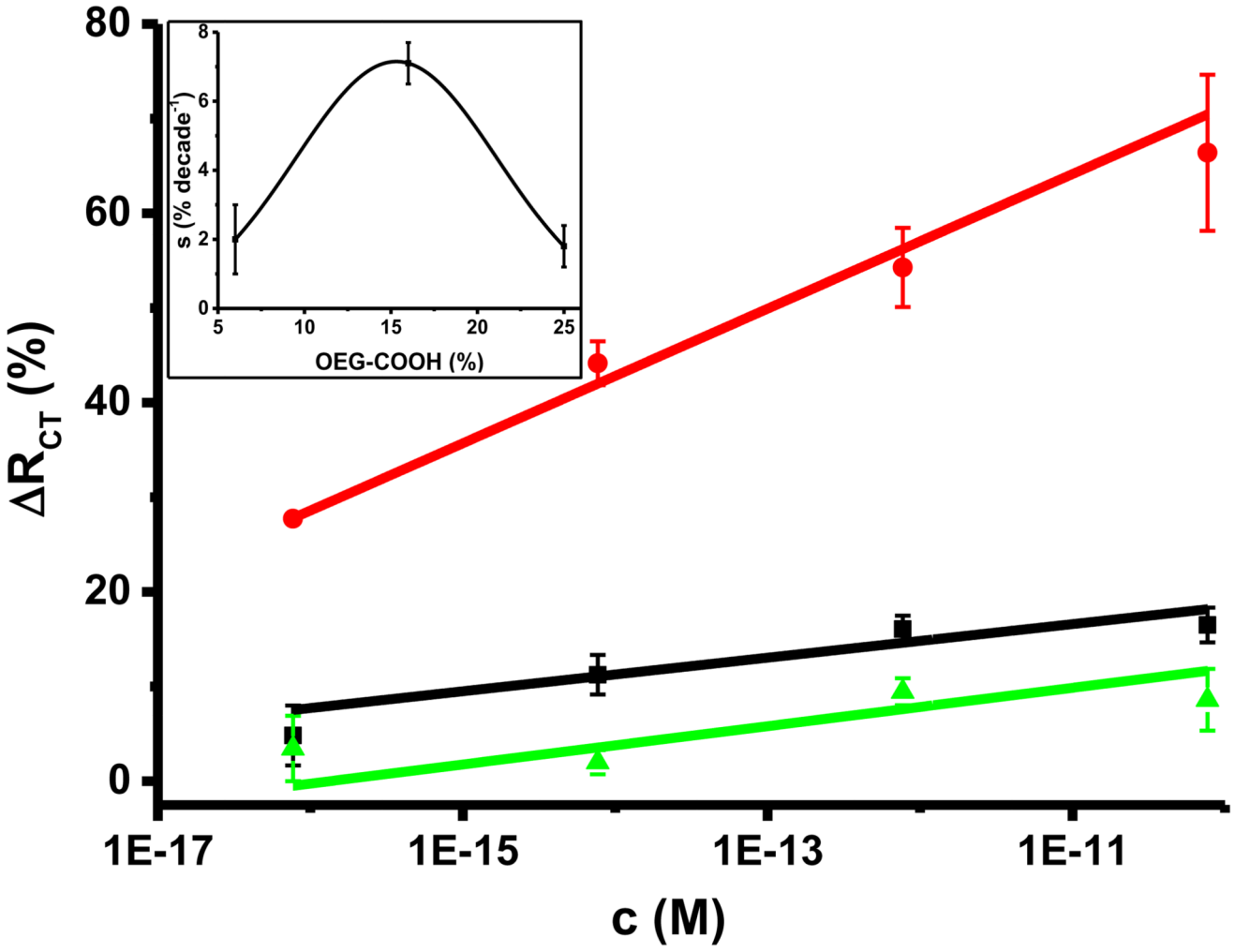

Figure 1.

Optimization of the composition of a mixed SAM layer composed of OEG-COOH and OEG ratio (black 1+3, red 1+5, green 1+15) with its influence on the sensitivity of detection of MAA lectin (analyte, inset figure) by the glycan biosensor. Calibration curves for *Maackia amurensis* agglutinin (MAA) detection by the glycan biosensors built up on a mixed SAM with three different composition are shown, as well. At least three independent electrodes were used for data generation.

Europe PMC Funders Author Manuscripts

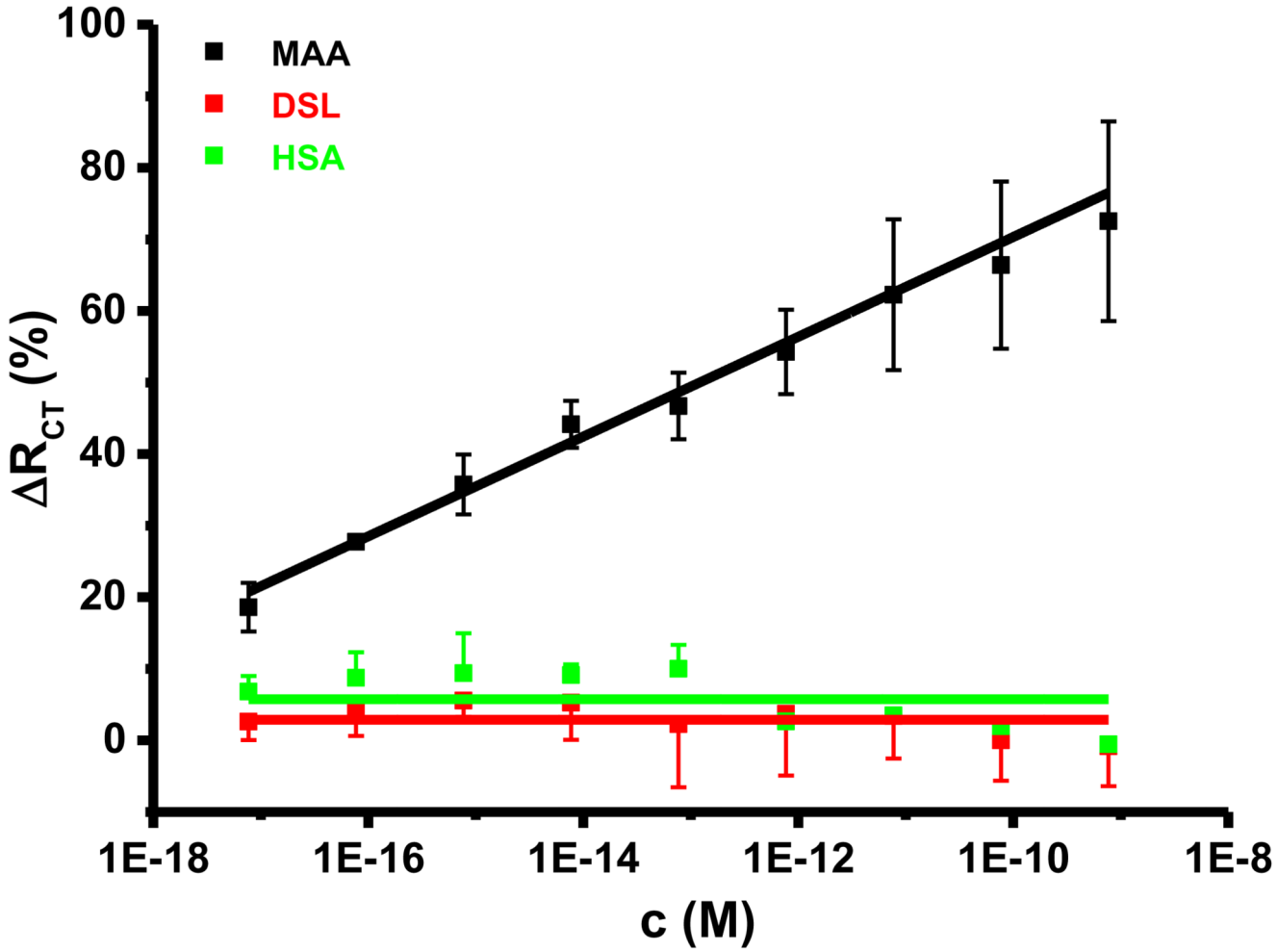

Figure 2.

Calibration of the glycan biosensor by two different lectins *Maackia amurensis* agglutinin (MAA, an analyte), *Datura stramonium* lectin (DSL) and human serum albumin (HSA).

Europe PMC Funders Author Manuscripts

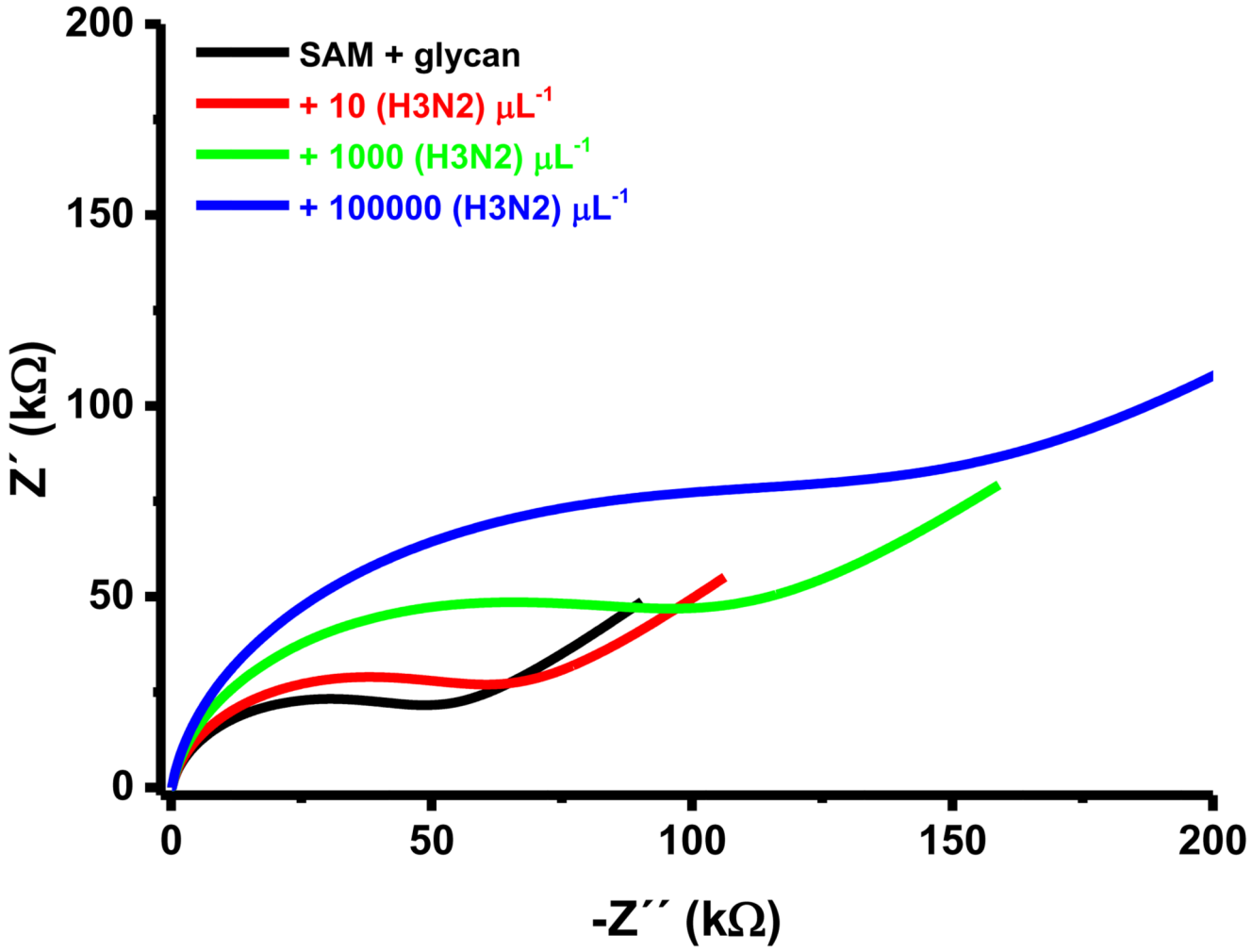

Figure 3.

Impedimetric characterization of the prepared glycan biosensor (SAM + glycan) and after interaction with increasing concentration of influenza H3N2 viral particles within a concentration range from 10 viral particles in 1 µl up to 100,000 viral particles in 1 µl. Data were fitted with an equivalent circuit shown in Scheme S2 with fitted parameters provided in Table S1 (both shown in the Supplementary information file).

Europe PMC Funders Author Manuscripts

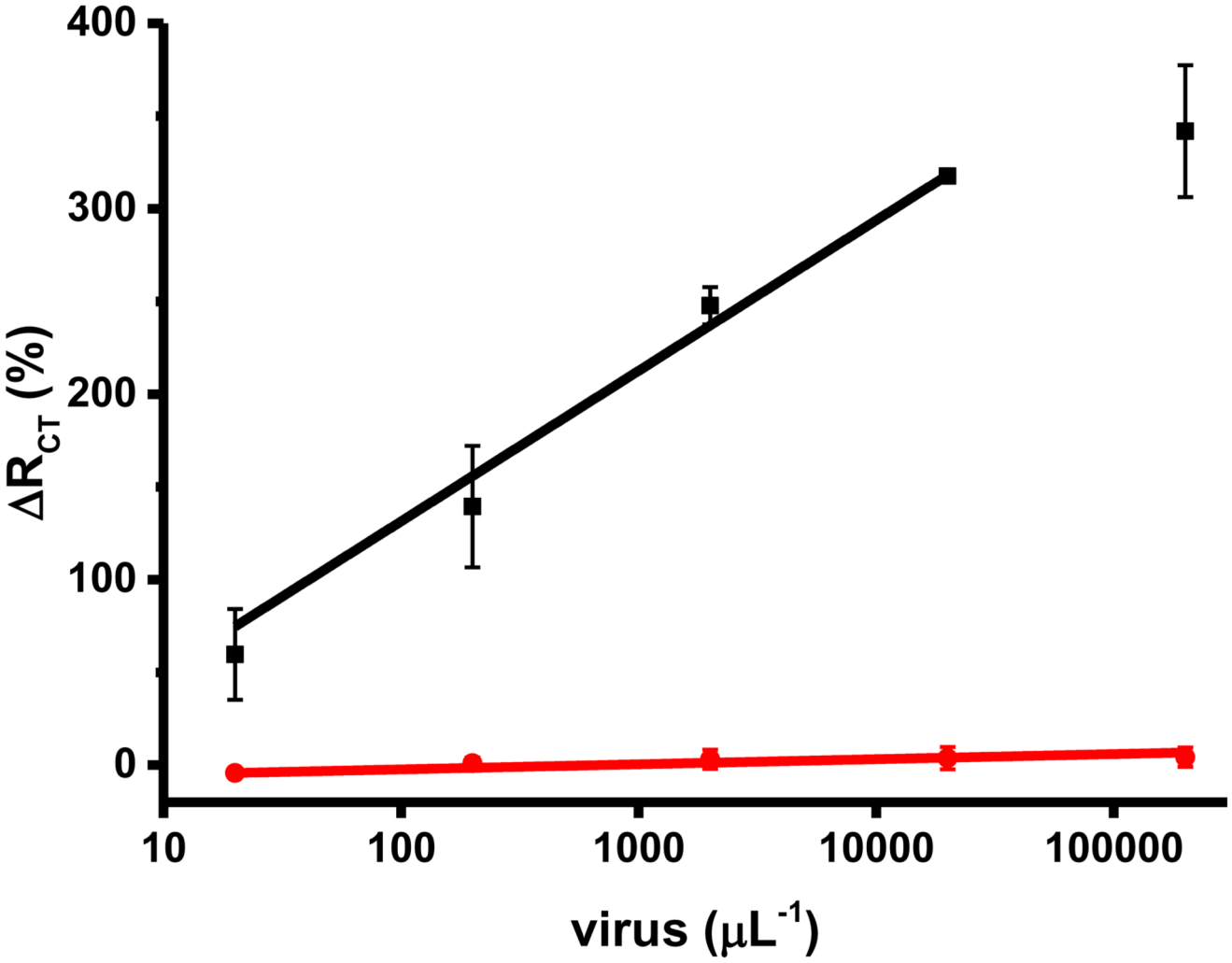

Figure 4.

Calibration curve for detection of influenza H3N2 viral particles (black, an analyte) and influenza H7N7 viral particles (red, a non-analyte).

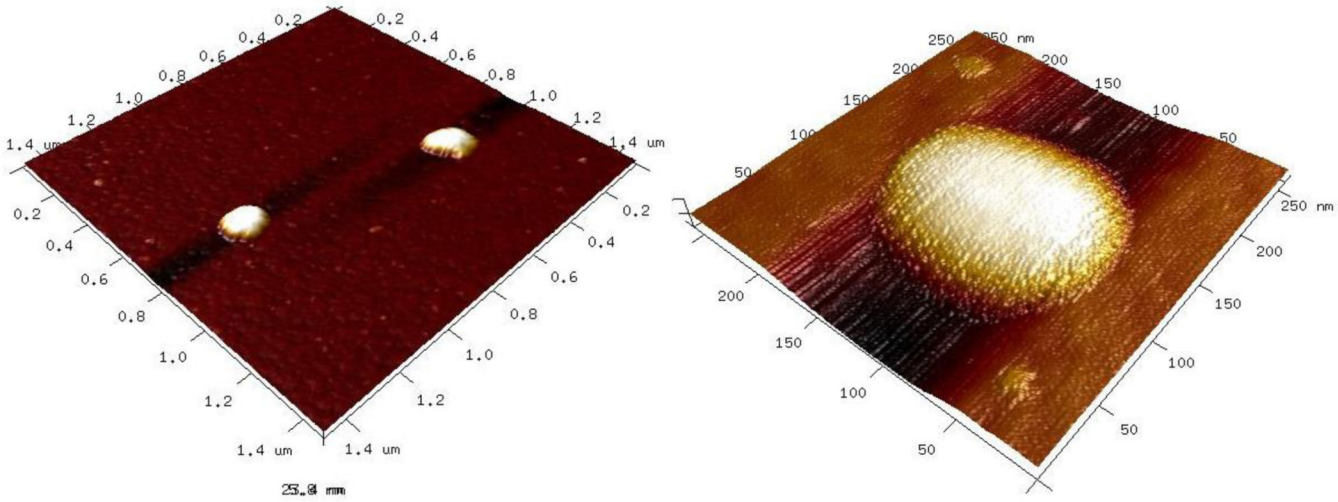

Figure 5.

AFM images of A) glycan biosensor + H3N2 virus 1.5 x 1.5 μm (z=35 nm), B) glycan biosensor + H3N2 virus 250 x 250 nm (z=37 nm).

Europe PMC Funders Author Manuscripts